


Ground-Based Microwave Radiometer Calibration: an Overview

Marcelo Miacci¹, Carlos Frederico Angelis¹

How to cite

Miacci M  <http://orcid.org/0000-0001-6912-5627>
Angelis CF  <http://orcid.org/0000-0003-0232-8280>

Miacci M; Angelis CF (2018) Ground-Based Microwave Radiometer Calibration: an Overview. J Aerosp Technol Manag, 10:e3518. doi: 10.5028/jatm.v10.927.

ABSTRACT: This paper intends to briefly present some basic concepts on the microwave radiometry and radiometer calibration research in remote sensing applications and demonstrate results and analysis of the cryogenic calibration of a microwave ground-based radiometer currently deployed in scientific campaigns in Brazil. The equipment described in this text operates at 22 – 30 GHz and at 51 – 59 GHz frequency ranges and uses as the calibration standard a target cooled by liquid nitrogen. Since an accurate calibration (with observation errors below 0.5 K) is important to provide confidence in the retrieval of vertical temperature and humidity profiles, this work aims also to comment on some effects of the errors in calibration procedure on the atmospheric parameters of interest.

KEYWORDS: Cryogenic calibration, Atmospheric profiling, Microwave radiometers, Ground-based radiometry

INTRODUCTION

A microwave radiometer is a passive device conceived for the detection of electromagnetic energy emitted by a source, a scene, or an object, since this energy has an inherent noise behavior. The spatial and spectral features of the observed sources determine the necessary specifications and performance of the sensor's subsystems.

Those subsystems include basically the antenna, a receiver and a power (or temperature) output monitor. In this context, the radiometer may be regarded as a highly sensitive calibrated microwave receiver operating under several environmental conditions in a wide temperature range.

Remote sensing of the microwave radiation of the atmosphere using ground-based radiometers has been proved highly efficient in a range of applications such as meteorology, weather forecast, *nowcasting*, telecommunications, astronomy, satellite and radar validation data, and so on (Miacci *et al.* 2015; Westwater *et al.* 2004; Godoy and Yung 1995; Janssen 1993; Ulaby *et al.* 1986; Hayes 1989). Those results also have contributed to the development and enhancements of radiative transfer models for clear and cloudy sky conditions.

These continuous advances in radiometry have been supported mainly by the use of sophisticated calibration techniques of the equipment, and also by employing primary temperature standards cooled by liquid nitrogen, that allows reasonable accuracy in sky measurements and, consequently, high relevance for meteorology (which is the main focus of this work).

Thus, radiometer measurement accuracy can be achieved by the correct and precise calibration of the receiver. The most common receiver calibration method is the two points or the hot-cold calibration, where the receiver input is terminated with two targets that are assumed to be ideal black bodies at their physical temperatures. For these primary standards, a microwave

¹Centro Nacional de Monitoramento e Alertas de Desastres Naturais – Cachoeira Paulista/SP – Brazil.

Correspondence author: Marcelo Miacci | Centro Nacional de Monitoramento e Alertas de Desastres Naturais | Rodovia Presidente Dutra, Km 40 | CEP: 12.630-000 – Cachoeira Paulista/SP – Brazil | E-mail: marcelo.miacci@cemaden.gov.br

Received: Jun. 8, 2017 | Accepted: Aug. 24, 2017

Section Editor: William Vaughan



absorber at room temperature and an absorber cooled with liquid nitrogen at ~77 K are generally employed (Miacci *et al.* 2015; Westwater *et al.* 2005).

This paper intends to briefly describe some theoretical basis, procedures and results on the cryogenic radiometer calibration technique performed at 22 – 30 GHz (K band) and 51 – 59 GHz (V band) frequency ranges (on the radiometer profiler model MP3000A developed by Radiometrics Corporation), and some considerations and technical details about analyzing calibration data for scientific campaigns carried out in Brazil (Miacci *et al.* 2015). A good review for other radiometer types, calibration methods, and applications can be found in Westwater *et al.* (2004).

BASIC PHYSICAL PRINCIPLES

From the ideal blackbody concept and the Kirchhoff's law, it is known that the energy emitted by a blackbody depends only on its physical temperature, in other words, the higher the temperature of the body (or medium) the greater the emission (Godoy and Yung 1995).

This statement was demonstrated through the spectral distribution calculation of the blackbody emission from the Planck's radiation law (Janssen 1993), which presents the radiance emitted by a blackbody at temperature T and frequency ν as (Eq. 1):

$$B_{\nu}(T) = \frac{2h\nu^3}{c^2} \frac{1}{(e^{h\nu/kT} - 1)} \quad (1)$$

where: $B_{\nu}(T)$ = radiance or blackbody spectral brightness ($\text{W m}^{-2} \text{sr}^{-1} \text{Hz}^{-1}$); h = Planck's constant ($6.63 \times 10^{-34} \text{ J s}$); ν = source frequency (Hz); c = light speed ($\sim 3 \times 10^8 \text{ m/s}$); k = Boltzmann's constant ($1.38 \times 10^{-23} \text{ J/K}$); T = source temperature (K).

Within the window of the electromagnetic spectrum where $h\nu \ll kT$ at temperature T , which is the case of the microwave region, the Eq. 1 reduces to the following equation given by the Rayleigh-Jeans law (Ulaby *et al.* 1986) (Eq. 2):

$$B_{\nu}(T) = \frac{2kT}{\lambda^2} = \frac{2\nu^2 kT}{c^2} \quad (2)$$

where: λ = wavelength (m).

Considering an antenna placed inside an anechoic chamber, which can be assumed approximately by a blackbody at temperature T , it can be concluded that the power received by the antenna terminals is frequency independent and related to the Johnson's noise power (Eq. 3):

$$P = kTdv \quad (3)$$

where: P = power emitted by the source (W); dv = frequency interval (Hz).

Finally, one can conclude that the noise power received by a radiometer could be described as an equivalent unit of blackbody temperature, thus enabling microwave radiometry as the key for measurement of microwave emissions (Hayes 1989).

THE RADIATIVE TRANSFER EQUATION

Through the basic considerations described herein, one could assume the emission of a real body as the ideal blackbody emitting at the same temperature.

If part of the incident energy from a given direction absorbed by the real body is expressed by $a(\nu)$, then the total emitted energy is $a(\nu)$. For an ideal lossless or reflector body, $a(\nu)$ is zero, and the incident energy is able to pass through the body without absorption or can be scattered to another direction of the space.

For a zenith-looking ground-based microwave radiometer observing a non-scattering scene, the equation that relates the brightness temperature, T_b , to the atmospheric state is the Radiative Transfer Equation (Eq. 4) (Westwater *et al.* 2005):

$$B_\nu(T_b) = B_\nu(T_c)e^{-\tau_\nu} + \int_0^\infty B_\nu(T(s))\alpha_\nu(s)e^{-\int_0^s \alpha_\nu(s')ds'} ds \quad (4)$$

where: s = distance (km); $T(s)$ = temperature (K) at the height s ; T_c = cosmic brightness temperature (~ 2.75 K); τ_ν = opacity in nepers (total optical depth or total attenuation through the path s), given by (Eq. 5):

$$\tau_\nu = \int_0^\infty \alpha_\nu(s) ds \quad (5)$$

where: $\alpha_\nu(s)$ = absorption coefficient (nepers/km) at s .

The use of the Eq. 4 is valid assuming the local thermodynamic equilibrium state (Godoy and Yung 1995).

ABSORPTION AND EMISSION AT THE MICROWAVE RANGE

The first studies on calculations of the water vapor and oxygen absorption continuum can be found in van Vleck (1947a; 1947b), along with the physical basis and experimental results leading to the improvements of the line-width calculations, including the work described in van Vleck and Weisskopf (1945) and Rosenkranz (1993).

The main sources of atmospheric microwave absorption and emission are the water vapor, oxygen and liquid water. In the 20 – 200 GHz frequency range, the absorption of microwaves by the water vapor arises at 22.235 GHz and at 183.3 GHz. The water vapor absorption continuum originates from high-frequency resonances that increase up to the infrared region.

Figure 1 shows a general water vapor absorption curve versus the operation frequency in the microwave spectrum.

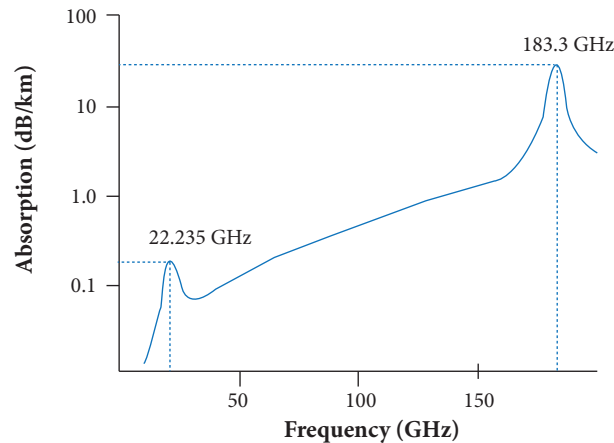


Figure 1. Water vapor absorption coefficient in the microwave range.

In the 2 – 200 GHz frequency range, the oxygen absorption rises at 60 GHz and at 118.75 GHz. For the pressure broadening effect (caused by molecular collisions) (Godoy and Yung 1995), there is a modification on the line-width shape for the water vapor and the oxygen absorption curves.

Figure 2 depicts a general oxygen absorption curve versus the operational frequency in the microwave range.

There are several microwave absorption models currently in use around the world for applications related to remote sensing and electromagnetic waves propagation research. One of the most used models is the Microwave Propagation Model (MPM) (Liebe and Layton 1987; Liebe *et al.* 1993). A comprehensive description of this model is found in (Rosenkranz 1998).

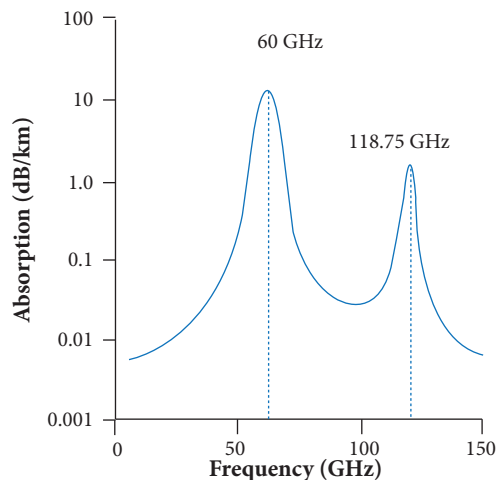


Figure 2. Oxygen absorption coefficient in the microwave range.

In the remote sensing research, the emission and absorption phenomena at microwaves frequency range are the main sources of data in order to retrieval atmospheric temperature and humidity profiles.

In Brazil, a microwave ground-based radiometer operating at the water vapor and oxygen lines (22 and 60 GHz bands) has been deployed to derive temperature and humidity profiles using a software based on artificial neural networks (provided by the radiometer's manufacturer) (Ware and Vandenberghe 2002; Solheim *et al.* 1998a), and the results of the measurements has recently supported several scientific campaigns over the country (Miacci *et al.* 2015).

RADIOMETER CALIBRATION

Radiometer calibration is an important task to ensure the system accuracy derived from the sky observations and, consequently, in retrieval of atmospheric parameters of interest. From the literature (Skou 1989), a calibration precision about 0.5 K is considered a good approach to obtain a minimum error in the sensor measurements.

There are two internal temperature standards involved in the measurements performed by the equipment described herein: noise sources (diodes), from which one can obtain the system gain, and a microwave absorber acting like a blackbody at room temperature. Thus the four-point noise injection method takes place.

In this method, a calibrated noise level (provided by the noise sources) is added to the observations of the sky and of the ambient internal target, to each microwave channel in order to get the required radiometer quasi-real-time self-calibration during the observations.

However, the assumption of perfect linearity of the receiver detector response, which is not true even under the square law operation, usually requires an absolute cryogenic calibration procedure in order to determine the right accurate values for the noise sources.

RADIOMETER MAIN CHARACTERISTICS

The radiometer described herein (MP3000A) performs atmospheric background radiation measurements in the microwave range. From those observations one can obtain temperature, water vapor, water liquid and humidity profiles which have been used mainly in weather forecast and *nowcasting* research (Cimini *et al.* 2015; Nadhulatha *et al.* 2013).

The profiles are retrieved using computational techniques like artificial neural networks with the advantage of a greater temporal sampling. However, there has been constant development in techniques aiming at enhancement of the profiles retrievals (Cimini *et al.* 2011; 2015; Xu *et al.* 2014; Sánchez *et al.* 2013; Frank *et al.* 2010).

The equipment has two built in microwave receivers, along with an antenna and a positioner system. The first receiver, designed for temperature profiling, primarily operates at frequencies ranging from 51 to 59 GHz. The second receiver, designed for water vapor and liquid profiling, operates at frequencies ranging from 22 to 30 GHz (Solheim *et al.* 1998b; Ware *et al.* 2003).

During its operation, the radiometer enables a calibrated signal through the noise sources, thus an accurate noise level is inserted at milliseconds intervals for all observations, providing the measurements of the system gain and the receiver self-calibration.

BRIGHTNESS TEMPERATURE TRANSFER FUNCTION

In the MP3000A radiometer there are associated parameters with each microwave channel, which are calibrated to provide the best accuracy over all the operational conditions. The parameters that require calibration remain stable for many years once they are calibrated in the factory over the nominal temperature range and normally require no adjustments.

Although the effective diode noise temperature (T_{nd}) is very stable, it must be calibrated periodically (once every six months) to assure the best accuracy in the measurements (Radiometrics Corporation 2008).

The radiometer employs a calibration algorithm and a procedure to obtain the sky brightness temperatures values (in K) from the measured level 0 values (raw data in Volts from the receiver output). This algorithm uses calibration coefficients in order to compensate the non-linearity effects of the system.

The transfer function used in this work is basically given by (Eq. 6):

$$T_{sky} = \left(\frac{V_{sky}}{G_{sky}} \right)^{\frac{1}{\alpha}} - T_{RX_sky} \quad (6)$$

where: T_{sky} = sky brightness temperature (K); V_{sky} = receiver output voltage from the sky observation with the noise diodes in off mode (V); G_{sky} = receiver gain during sky observation (V/K); α = non-linearity correction exponent (dimensionless); T_{RX_sky} = receiver noise temperature during sky observation (K).

From the level 0 data plus the calibration parameters and the values directly measured by the radiometer receiver, the brightness temperatures from observations can be reached. More details on the transfer function can be found in Radiometrics Corporation (2008).

CALIBRATION TARGETS

Applying the background of the radiation theory, one could consider as a blackbody a microwave load with a high return loss value (usually greater than 40 dB) since its noise temperature will be close to its physical temperature (Ulaby *et al.* 1986). Thus, a useful procedure for a radiometer calibration is to connect a cooled microwave load (with a well-known temperature) to the radiometer terminals.

It is common to cool down the loads at cryogenic temperatures by its submersion in a liquid helium medium (Trembath *et al.* 1968), or in a liquid nitrogen medium (Hardy 1973).

An alternative procedure could be a target, such as a cooled microwave absorber, positioned in front a radiometer antenna. In that way, the emission of the target (or brightness temperature) will be close to its physical temperature as well, thus the radiation could be detected by the antenna.

Some of the electromagnetic characteristics of targets cooled with liquid nitrogen for cryogenic calibrations and the main errors involved can be found in Rose *et al.* (2005) and Randa *et al.* (2005).

In the present work, another arrangement was deployed with the cryogenic target positioned over the radiometer antenna (Fig. 3), but there are other procedures that could be used, such as the radiometer side-mounted target, used by Löhnert and Maier (2012) and by Pospichal *et al.* (2012).

In Fig. 3, it is observed that the temperature of the calibration standard will be the same of the liquid nitrogen, but other parameters must to be considered to perform an accurate receiver calibration.

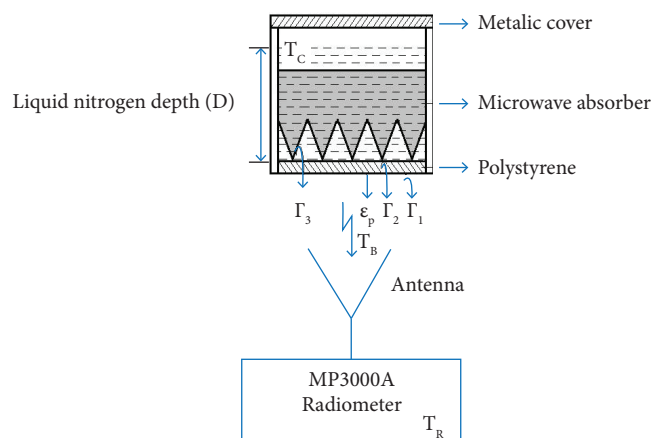


Figure 3. Basic set-up of the cryogenic target to the radiometer calibration.

The first parameter to be considered is the emissivity of the target ϵ , and alternatively, its reflection coefficient $1 - \epsilon$. Assuming the cryogenic target within a liquid nitrogen medium at $T_C = 77\text{ K}$, and assuming the emitted radiometer temperature $T_R = 300\text{ K}$, the measured brightness temperature (T_B) will be (Eq. 7):

$$T_B = T_C \cdot \epsilon + T_R \cdot (1 - \epsilon) \quad (7)$$

And the error (Δ) will be given by Eq. 8:

$$\Delta = (T_R - T_C) \cdot (1 - \epsilon) \quad (8)$$

The second parameter is the liquid nitrogen boiling point, which is dependent of the local pressure given by (Eq. 9) (Radiometrics Corporation 2008):

$$T_{LN} = 68.23 + 0.009037P \quad (9)$$

where: T_{LN} = liquid nitrogen boiling point (K); P = room barometric pressure (mb).

The third parameter is the hydrostatic load taken from the liquid nitrogen depth inside the cryogenic target ($\sim 1.2\text{ mb/cm}$). For example, in operational conditions the real temperature of the target could be increased by values greater than 0.15 K for a nitrogen depth of 15 cm or more.

There are still other parameters that must to be taken into account, according to Fig. 3 (Hewison and Gaffard 2003): insertion loss of the target insulation (ϵ_p); reflection coefficient of air/insulation interface (Γ_1), insulation/LN2 interface (Γ_2) and absorber/LN2 interface (Γ_3).

For instance, considering the aforementioned effects, it is possible to get an increase of approximately 2.0 to 3.0 K from the estimated temperature of the liquid nitrogen, which could invalidate the radiometer calibration (Miacci *et al.* 2015).

ASSESSMENT OF A RADIOMETER CALIBRATION

An example of a cryogenic calibration of the radiometer is given in order to demonstrate the verification of the noise sources and to check both the calibration algorithm (implemented in the radiometer to correct non-linearity effects), and the transfer function to derive sky brightness temperature from the receiver detector output voltage. More in-depth information about this calibration is available in Miacci *et al.* (2015).

The radiometer used in this work (MP3000A by Radiometrics Corporation) is shown in Fig. 4a and the cryogenic target without the liquid nitrogen is shown in Fig. 4b.

For the calibration procedure, the target must be installed over the radiometer (Fig. 5), and after that the automated computer routines (provided by the instrument manufacturer) are executed.

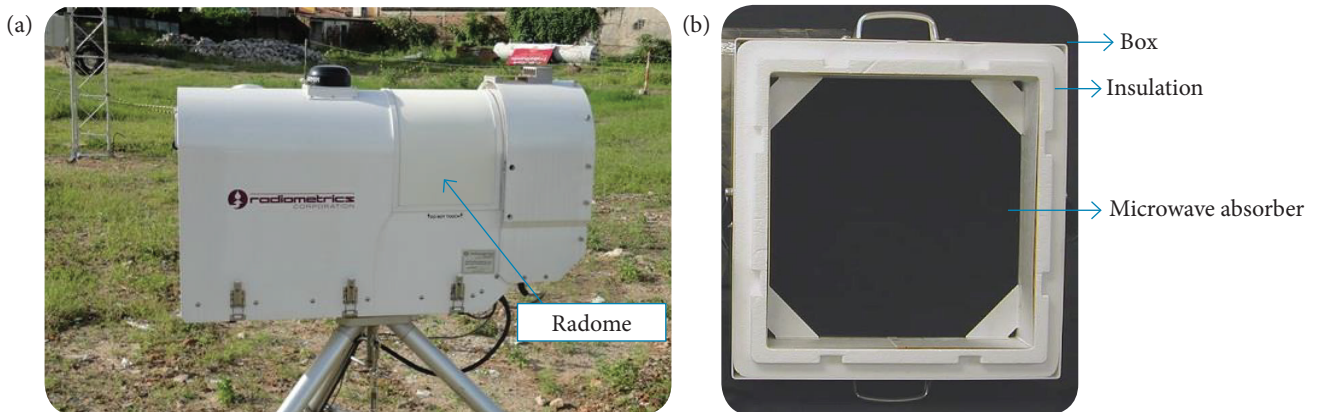


Figure 4. (a) Radiometer model MP3000A; (b) Target box.

During calibration, the control software displays the elapsed time and a calibration data graph of the noise temperature diodes (Tnd) for each channel. When calibration is complete the new Tnd values are recorded for all channels.

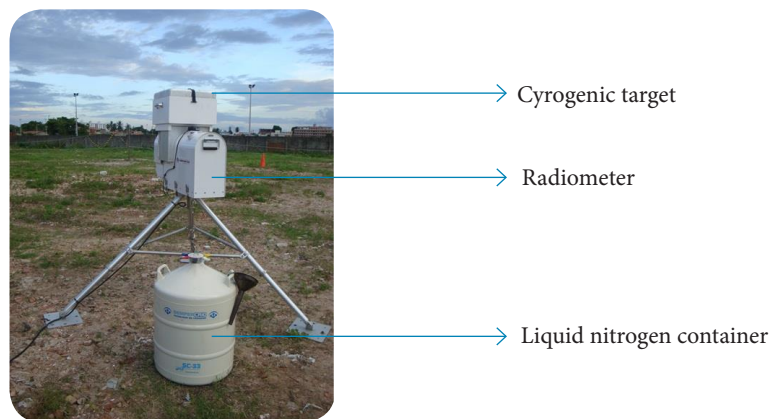


Figure 5. Set-up for the calibration of the microwave radiometer.

The control computer runs an application that measures alternately the emission of the internal ambient target and the external target through the variation of the antenna pointing angle inside the radiometer cabinet. Thus the brightness temperatures of the targets are recorded for the selected microwave channels and these values must be close to the employed standard targets.

To check the calibration, it is necessary to inspect the curves of Tnd (noise temperature of the diodes). These values should be fairly constant in amplitude, as shown in Figs. 6 and 7 for the K and V bands. Those results indicate that a high confidence calibration can be achieved.

Figure 8 illustrates the curves for calibration verification for all channels for the internal ambient target. The curves are well arranged over a reference level (~ 313.5 K) and do not depart far from this average, mainly because there are no interfaces between the target and the radiometer antenna.

Figure 9 shows the calibration curves for all channels for the cryogenic target. Due to the reflections and the losses described in Radiometer Calibration section, there is a difference between the average in the K-band calibration curves and the V-band

curves. So these differences must be taken into account in order to assure a good calibration, with the same nominal cryogenic target temperature measurements for all the microwave channels.

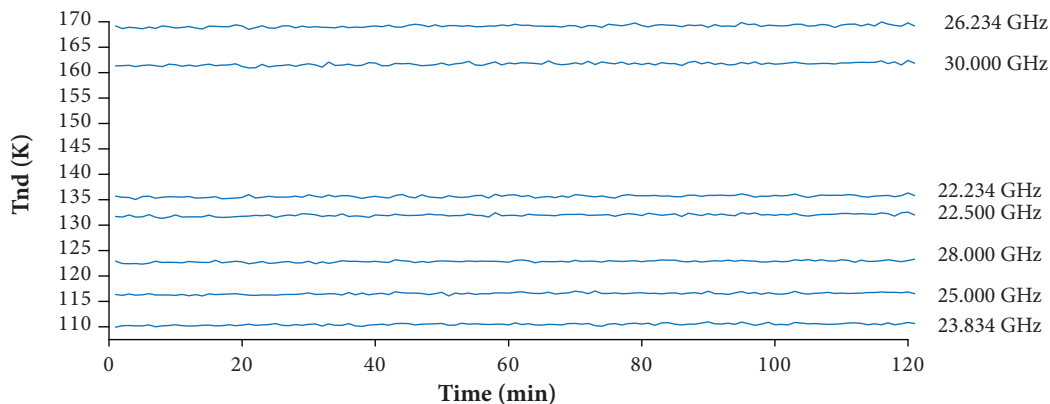


Figure 6. Verification test of the noise diodes calibration for the K band channels.

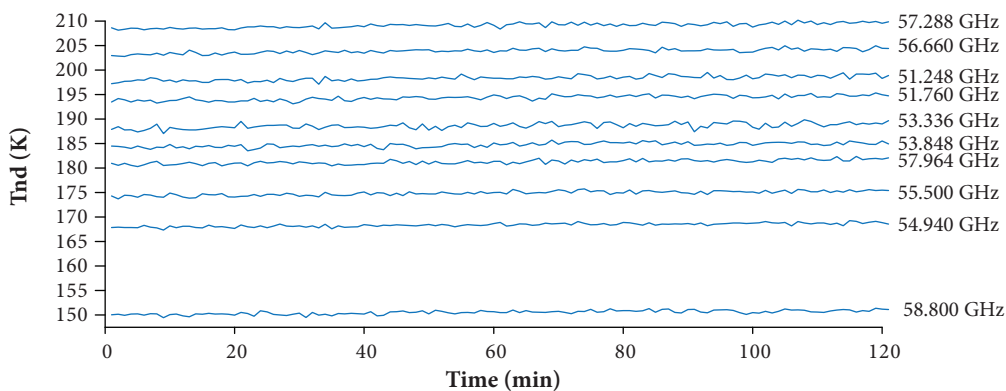


Figure 7. Verification test of the noise diodes calibration for the V band channels.

Other effects, like the calibration temperature modulation associated with standing waves, and liquid nitrogen evaporation, are reported for side-mounted cryogenic calibration (Randa *et al.* 2005).

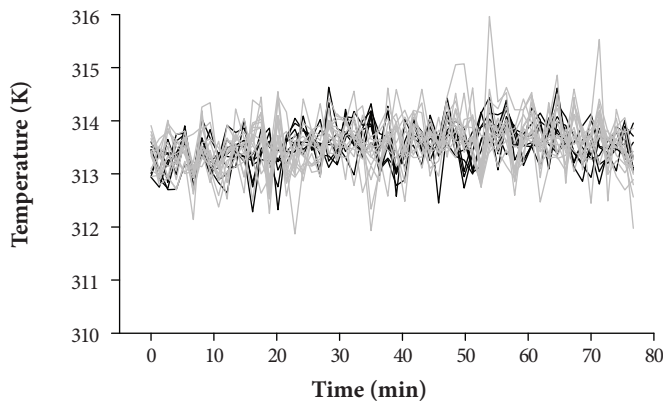


Figure 8. Brightness temperature of the internal ambient target for all radiometer channels [K-Band in black and V-Band in gray].

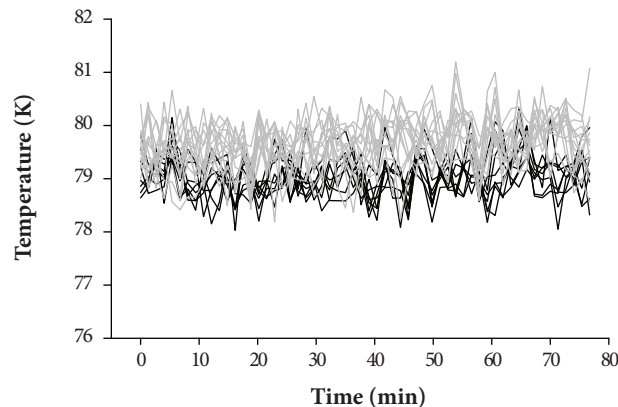


Figure 9. Brightness temperature of the cryogenic target for all radiometer channels (K-Band in black and V-Band in gray).

Assuming 0.5 K calibration accuracy, integrated water vapor and cloud liquid water path can be obtained with 0.5 kg m^{-2} and 20 g m^{-2} accuracy (Pospichal *et al.* 2012), the retrieved accuracy for temperature profile is 0.5 K near surface increasing to 1.5 K at 5 km, and for humidity profile is not more than 1 g m^{-3} at all altitudes (Hewison and Gaffard 2003; WMO 2008; Güldner and Spänkuch 2001; Hewison 2007).

For instance, Fig. 10 depicts a generic comparison between radiosonde and radiometer temperature profiles, based on data from a campaign in the Brazil's northeast (CHUVA Science Team 2010), and the root mean square errors.

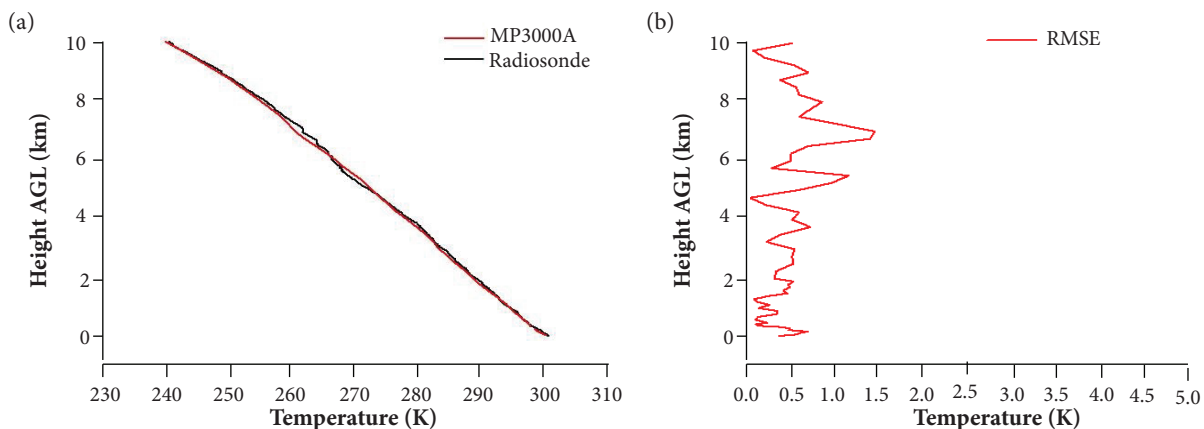


Figure 10. Radiometer temperature profiles retrieved as compared to (a) a radiosonde; and (b) RMS difference.

In Fig. 10, the temporal resolution of the radiometer is about 2 min and the rise time of the radiosonde is about 40 min. For the presented comparison purposes, an average of multiple radiometer profiles (in an elapsed time of 40 min) is compared to a single radiosonde launch at the same period and location.

For the humidity profiles are expected errors of approximately 5 up to 25% depending on the altitude – a greater error at high altitudes due to radiometer's spatial resolution and artificial neural networks technique employed. More information about the experiments is found in CHUVA Science Team (2010).

According to Hewison and McGrath (2001), there are still other parameters that could be considered for in the calibration if the radiometer operational frequency range is above 60 GHz, like scattering of dielectric components of the calibration target.

CONCLUSION

This study briefly presented some basic concepts revisited from the literature produced all over the years on the radiometry research and some results and analysis of the cryogenic calibration of a microwave ground-based radiometer currently deployed in field campaigns over Brazil.

The accuracy of the calibration performed and the results of the profile retrievals compared with radiosondes proves microwave radiometry as an alternative technique for atmospheric profiling with the advantage of greater temporal resolution (retrievals every ~2 min).

Microwave radiometry is a field where the researchers and the radiometer manufacturers are constantly providing promising results for the enhancement of brightness temperature measurements and retrieval of atmospheric profiles, along with other calibration techniques that has been applied, such as the tipping curve (Han and Westwater 2000) and even improvements in computational techniques.

AUTHOR'S CONTRIBUTION

Conceptualization, Miacci M; Methodology, Miacci M; Investigation, Miacci M and Angelis C; Writing – Original Draft, Miacci M; Writing – Review and Editing, Miacci M and Angelis C; Funding Acquisition, Angelis C; Resources, Angelis C; Supervision, Angelis C.

ACKNOWLEDGMENTS

The authors wish to thank the CHUVA project team for the technical support. This work was supported by the Sao Paulo Research Foundation (FAPESP), grant 09/15235-8 and 11/03093-4 and by the National Council for Science and Technology Development (CNPq), grant 300153/2016-3 and 372788/2017-3.

REFERENCES

- CHUVA Science Team (2010) Cloud processes of the main precipitation systems in Brazil: A contribution to cloud resolving modeling and to the GPM (Global Precipitation Measurement); [accessed 2017 June 6]. <http://chuvaproject.cptec.inpe.br/>
- Cimini D, Campos E, Ware R, Albers S, Giuliani G, DREAMUNO J, Joe P, Koch SE, Cober S, Westwater E (2011) Thermodynamic atmospheric profiling during the 2010 winter olympics using ground-based microwave radiometry. *IEEE Transactions on Geoscience and Remote Sensing* 49(12):4959-4969. doi: [http://10.1109/TGRS.2011.2154337](http://dx.doi.org/10.1109/TGRS.2011.2154337)
- Cimini D, Nelson M, Güldner J, Ware R (2015) Forecast indices from ground-based microwave radiometer for operational meteorology. *Atmos Meas Tech* 8:315-333. doi: [10.5194/amt-8-315-2015](http://dx.doi.org/10.5194/amt-8-315-2015)
- Goody RM, Yung YL (1995) Atmospheric radiation, theoretical basis. 2nd ed. New York: Oxford University Press.
- Güldner J, Spänkuch D (2001) Remote sensing of the thermodynamic state of the atmospheric boundary layer by ground-based microwave radiometry. *J Atmos Oceanic Technol* 18:925-933. doi: [10.1175/1520-0426\(2001\)018<0925:RSOTTS>2.0.CO;2](http://dx.doi.org/10.1175/1520-0426(2001)018<0925:RSOTTS>2.0.CO;2)
- Han Y, Westwater ER (2000) Analysis and improvement of tipping calibration for ground-based microwave radiometers. *IEEE Trans Geoscience and Remote Sensing* 38(3):1260-1276. doi: [10.1109/36.843018](http://dx.doi.org/10.1109/36.843018)
- Hardy WN (1973) Precision Temperature reference for microwave radiometry. *IEEE Trans on Microwave Theory and Techniques* 21(3):149-150. doi: [10.1109/TMTT.1973.1127954](http://dx.doi.org/10.1109/TMTT.1973.1127954)
- Hayes RD (1989) Radiometric measurements. In: Currie NC, editor. Radar reflectivity measurement: techniques and applications. Norwood: Artech House. p. 715-739.

- Hewison TJ (2007) 1D-VAR retrieval of temperature and humidity profiles from a ground-based microwave radiometer. *Trans on Geoscience and Remote Sensing* 45(7):2163-2168. doi: 10.1109/TGRS.2007.898091
- Hewison T, Gaffard C (2003) Radiometrics MP3000 microwave radiometer performance assessment. (TR29). UK Met Office Technical Report.
- Hewison T, McGrath AJ (2001) Performance assessment of liquid nitrogen calibration target supplied by Fred Solheim (Radiometrics) at 89, 157 and 183 GHz. (Technical Note 39). MRF Technical Note.
- Janssen MA (1993) An introduction to the passive remote sensing of atmospheres. New York: John Wiley & Sons. Atmospheric remote sensing by microwave radiometry; p.1-36.
- Liebe HJ, Hufford GA, Cotton MG (1993) Propagation modeling of moist air and suspended water/ice particles at frequencies below 1000 GHz. Presented at: AGARD Conference 1993. AGARD Conference Proceedings 542, Atmospheric propagation effects through natural and man-made obscurants for visible through mm-wave radiation; Mallorca, Spain.
- Liebe HJ, Layton DH (1987) Millimeter wave properties of the atmosphere: laboratory studies and propagation modeling. (TR-87-224). NTIA Technical Report.
- Löhnert U, Maier O (2012) Operational profiling of temperature using ground-based microwave radiometry at Payerne: prospects and challenges. *Atmos Meas Tech* 5:1121-1134. doi: 10.5194/amt-5-1121-2012
- Madhulatha A, Rajeevan M, Ratnam MV, Bhate J, Naidu CV (2013) Nowcasting severe convective activity over southeast India using ground-based microwave radiometer observations. *Journal of Geophysical Research* 118(1):1-13. doi: 10.1029/2012JD018174
- Marzano FS, Cimini D, Montopoli M (2010) Investigating precipitation microphysics using ground-based microwave remote sensors and disdrometer data. *Atmospheric Research* 97(4):583-600. doi: 10.1016/j.atmosres.2010.03.019
- Miacci MAS, Angelis CF, Calheiros AJR, Machado LAT (2015) Some considerations on the cryogenic calibration technique for microwave and millimeter wave ground-based radiometry. *Revista de Gestão & Tecnologia* 3(3):47-52.
- Pospichal B, Maschwitz G, Kuchler N, Rose T (2012) Standing wave patterns at liquid nitrogen calibration of microwave radiometers. Presented at: 9th International Symposium on Tropospheric Profiling (ISTP). Proceedings of the 9th ISTP; L'Aquila, Italy.
- Radiometrics Corporation (2008) MP3000A Profiler Operator's Manual. Boulder, USA.
- Randa J, Walker DK, Cox AE, Billinger RL (2005) Errors resulting from the reflectivity of calibration targets. *IEEE Trans on Geoscience and Remote Sensing* 43(1):50-58. doi: 10.1109/TGRS.2004.839809
- Rose T, Crewell S, Löhnert U, Simmer C (2005) A network suitable microwave radiometer for operational monitoring of the cloudy atmosphere. *Atmospheric Research* 75(3):183-200. doi: 10.1016/j.atmosres.2004.12.005
- Rosenkranz PW (1993) Absorption of microwaves by atmospheric gases. In: Janssen MA, editor. Atmospheric remote sensing by microwave radiometry. New York: John Wiley & Sons. p. 37-90.
- Rosenkranz PW (1998) Water vapor microwave continuum absorption: a comparison of measurements and models. *Radio Science* 33(4):919-928. doi: 10.1029/98RS01182
- Sánchez JL, Posada R, García-Ortega E, López L, Marcos JL (2013) A method to improve the accuracy of continuous measuring of vertical profiles of temperature and water vapor density by means of a ground-based microwave radiometer. *Atmospheric Research* 122:43-54. doi: 10.1016/j.atmosres.2012.10.024
- Skou N (1989) *Microwave Radiometer Systems: Design and Analysis*. Norwood: Artech House.
- Solheim F, Godwin J, Ware R (1998) Passive ground-based remote sensing of atmospheric temperature, water vapor, and cloud liquid water profiles by a frequency synthesized microwave radiometer. *Meteorologische Zeitschrift* 7(6):370-376.
- Solheim F, Godwin JR, Westwater ER, Han Y, Keihm SJ, Marsh K, Ware R (1998) Radiometric profiling of temperature, water vapor, and liquid water using various inversion methods. *Radio Sci* 33(2):393-404. doi: 10.1029/97RS03656
- Trembath CL, Wait DF, Engen GF, Foote WJ (1968) A low-temperature microwave noise standard. *IEEE Trans on Microwave Theory and Techniques* 16(9):709-714. doi: 10.1109/TMTT.1968.1126775
- Ulaby FT, Moore RK, Fung AK (1986) *Microwave remote sensing, active and passive – microwave remote sensing fundamentals and radiometry*. v 1. Norwood: Artech House.
- van Vleck JH (1947a) The absorption of microwaves by uncondensed water vapor. *Physical Review* 71(7):425-433. doi: 10.1103/PhysRev.71.425
- van Vleck JH (1947b) The absorption of microwaves by oxygen. *Physical Review* 71(7):413-424. doi: 10.1103/PhysRev.71.413
- van Vleck JH, Weisskopf VF (1945) On the shape of collision-broadened lines. *Reviews of Modern Physics* 17(2-3):227-236. doi: 10.1103/RevModPhys.17.227

Ware R, Carpenter R, Güldner J, Liljegren J, Nehrkorn T, Solheim F, Vandenberghe F (2003) A multi-channel radiometric profiler of temperature, humidity, and cloud liquid. *Radio Sci* 38(4):8079. doi: 10.1029/2002RS002856

Ware R, Vandenberghe F (2002) Radiometric profiling of tropospheric temperature, humidity and cloud liquid. Presented at: World Meteorological Organization Technical Conference (TECO-2002). Proceedings of TECO-2002; Bratislava, Slovakia.

Westwater ER, Crewell S, Mätzler C (2004) A Review of surface-based microwave and millimeter-wave radiometric remote sensing of the troposphere. *Radio Science Bulletin of URSI* 310:59-80. doi: 10.23919/URSIRSB.2004.7909438

Westwater R, Crewell S, Mätzler C (2005) Surface-based microwave and millimeter wave radiometric remote sensing of the troposphere: a tutorial. *IEEE Geoscience and Remote Sensing Society Newsletter* March: 16-33.

WMO (2008) Guide to meteorological instruments and methods of observation WMO-No. 8. Geneva: WMO.

Xu G, Ware R, Zhang W, Feng G, Liao K, Liu Y (2014) Effect of off-zenith observation on reducing the impact of precipitation on ground-based microwave radiometer measurement accuracy in Wuhan. *Atmospheric Research* 140-141:85-94. doi: 10.1016/j.atmosres.2014.01.021